



Received July 03, 2025; accepted August 12, 2025; Date of publication September 03, 2025.
 The review of this paper was arranged by Associate Editor Edivan L. C. da Silva[✉] and Editor-in-Chief Heverton A. Pereira[✉].

Digital Object Identifier <http://doi.org/10.18618/REP.e202552>

Cryogenic DC-DC Boost Converter Employing Superconducting Inductor

Samir A. Mussa^{✉1,*}, Herminio M. de Oliveira Filho^{✉2}, Gustavo A. L. Henn^{✉2},
 Douglas M. Sotoriva^{✉1}, Lauro Ferreira^{✉3}, Loïc Quéval^{✉3}

¹Universidade Federal de Santa Catarina, Instituto de Eletrônica de Potência, Florianópolis – SC, Brazil.

²Universidade da Integração Internacional da Lusofonia Afrobrasileira, Instituto de Engenharias e Desenvolvimento Sustentável, Redenção – CE, Brazil.

³Université Paris-Saclay, CentraleSupélec, CNRS, GeePS, Gif-sur-Yvette, France.

e-mail: samir@inep.ufsc.br^{*}; herminio@unilab.edu.br; gustavo@unilab.edu.br; douglas.sotoriva@outlook.com; lauro.fsn1@gmail.com; loic.queval@gmail.com.

^{*} Corresponding author.

ABSTRACT

Cryogenic power electronics applications, commonly referred to as cryo-converters, offer key advantages over conventional ambient-temperature systems, including higher power density and improved efficiency. This paper presents the experimental analysis of a prototype cryogenic boost converter (cryoboost) operating in continuous conduction mode (CCM), under both room-temperature and cryogenic conditions. The study focuses on the voltage gain behavior. Two different inductors were tested and compared: an air-core copper coil and a high-temperature superconducting (HTS) air-core inductor (BSCCO pancake coil, 4 mm tape). Experimental results demonstrate that the HTS inductor operating at cryogenic temperatures significantly enhances the voltage gain compared to the copper inductor at room temperature. These findings suggest that HTS-based inductors are a promising alternative for high-gain DC-DC converter applications in cryogenic environments.

KEYWORDS DC-DC boost converter, HTS coil, cryogenic converter, cryoboost, superconductors.

I. INTRODUCTION

The increasing adoption of renewable energy sources has heightened the demand for efficient DC–DC converters, particularly in photovoltaic systems. To maximize energy extraction, Maximum Power Point Tracking (MPPT) controllers are commonly implemented in both grid-connected and off-grid configurations [1].

DC–DC converters are also extensively used in a variety of applications, including solar energy systems, aeronautics [2], space systems [3], uninterruptible power supplies (UPS), modern data centers [4], battery backup systems, distributed power architectures, and battery-powered platforms. They also play a crucial role in fuel cell systems, electric vehicles (EVs), and hybrid electric vehicles (HEVs).

Numerous studies have investigated topologies for high-gain static DC–DC converters. Notable contributions include the works of [5]–[8], as well as the seminal design proposed by Middlebrook [9], which laid the foundation for early high-gain converter architectures.

In isolated DC–DC converters, high-frequency switched transformers are commonly employed to achieve voltage step-up. This approach offers advantages such as reduced size and weight, electrical isolation for enhanced safety, and design flexibility, including support for multiple outputs and isolated ground references [10]–[12].

Non-isolated converters, by eliminating the transformer, offer benefits such as lower cost, reduced size, higher efficiency, and simpler topologies compared to isolated designs

[13]–[19]. To achieve high voltage gain in these converters, several techniques have been developed and can be broadly classified into seven categories: cascading of two DC–DC converters, switched-capacitor networks, voltage multipliers, switched inductors, magnetic coupling, multilevel converters, and differential converter structures [20]–[22].

This work investigates a promising approach for implementing a non-isolated high-gain static converter by leveraging the enhanced performance of components under cryogenic conditions. Cryogenic operation enables the use of superconducting magnetic elements and improves semiconductor behavior, resulting in reduced conduction and switching losses, optimized threshold voltages, and overall improvements in efficiency. Furthermore, by operating at cryogenic temperatures, two significant factors can be exploited to further decrease the inductor resistance (R_L): the use of superconducting coils for the inductor and the adoption of components that exhibit reduced conduction losses at these temperatures.

Cryogenic power electronics have gained increasing interest in applications where high efficiency, compactness, and extreme operating conditions are required. Notable examples include space systems [23], high-energy physics and fusion devices [24], quantum computing platforms [25], and superconducting magnetic energy storage (SMES) systems [26]. In such scenarios, cryogenic temperatures enable the use of superconducting components, drastically reducing resistive losses and allowing high current densities

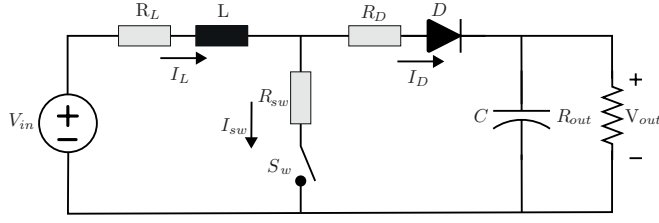


FIGURE 1. Considering some of the non-ideal aspects of a Boost converter's DC-DC operation.

in magnetic elements. Additionally, power semiconductor devices—particularly wide bandgap technologies such as SiC and GaN—exhibit improved cryogenic performance, including reduced on-state resistance, lower leakage currents, enhanced carrier mobility, and superior switching behavior [27]–[29]. These advantages have motivated the investigation of unconventional passive components, including air-core and high-temperature superconductor (HTS)-based inductors. Air-core inductors eliminate ferromagnetic losses and magnetic saturation, offering stable performance at high frequencies, especially in applications where weight and magnetic linearity are critical [30]. HTS inductors, typically based on REBCO tapes, enable compact, low-loss magnetics with high current handling, and are being explored in energy storage, protection devices, and power converters [31], [32]. While not yet widespread in conventional designs, these technologies present compelling benefits for cryogenic power converters targeting extreme-performance domains.

II. IMPACT OF INDUCTOR COPPER LOSSES ON THE BOOST CONVERTER VOLTAGE GAIN

This analysis considers a conventional DC-DC boost converter, as illustrated in Fig. 1, at room temperature. It consists of a DC input voltage source V_{in} , an inductor L , a semiconductor switch S_w , a diode D , an output capacitor C , and a load resistor R_{out} . In continuous conduction mode (CCM) and a switching period T_s , the converter operates in two distinct stages. During the first stage, the switch S_w is turned on, and the inductor is charged. In the second stage, the switch is turned off, discharging the inductor's previously stored energy through the load. The duration of each stage is determined by the duty cycle d . The static voltage gain G is given by:

$$G = \frac{V_{out}}{V_{in}} = \frac{1}{1-d} \quad (1)$$

Non-ideal components introduce losses that effectively limit the voltage gain. These power losses can be modeled by incorporating series resistances with each component. Specifically, conduction losses are represented by resistive elements, denoted as R_L , R_{sw} , and R_D , [33].

By including the inductor copper losses (R_L) in the model, the inductor voltage $v_L(t)$ and the output capacitor current $i_C(t)$ during the first stage ($0 \leq t \leq d \cdot T_s$) can be expressed

by (2) and (3), respectively. During the second stage ($d \cdot T_s \leq t \leq T_s$), these variables are given by (4) and (5).

$$v_L(t) = V_{in} - R_{out} \cdot I_L \quad (2)$$

$$i_C(t) = -\frac{V_{out}}{R_{out}} \quad (3)$$

$$v_L(t) = V_{in} - I_L \cdot R_{out} - V_o \quad (4)$$

$$i_C(t) = I_L - \frac{V_{out}}{R_{out}} \quad (5)$$

where I_L is the average inductor current. Since the ripple components of $v_{out}(t)$ and $i_L(t)$ are small compared to their DC values, they are approximated as $v_{out}(t) \approx V_{out}$ and $i_L(t) \approx I_L$.

By applying the inductor voltage-second balance to equations (2) and (4), the expression in (6) is obtained. Similarly, applying the capacitor charge balance to equations (3) and (5) results in equation (9).

$$\frac{1}{T_s} \int_0^{T_s} v_L(t) dt = V_{in} - I_L R_{out} - (1-d)V_{out} = 0 \quad (6)$$

$$\frac{1}{T_s} \int_0^{T_s} i_C(t) dt = (1-d)I_L - \frac{V_{out}}{R_{out}} = 0 \quad (7)$$

By rearranging equations (6) and (9), the static voltage gain of the boost converter can be expressed as shown in equation (8). This expression comprises two components: the first term corresponds to the ideal voltage gain, while the second term represents the attenuation caused by the inductor's copper losses included in the model.

$$G = \frac{V_{out}}{V_{in}} = \left(\frac{1}{1-d} \right) \left(\frac{1}{1 + \frac{R_L}{R_{out}(1-d)^2}} \right) \quad (8)$$

Although the model assumes a constant inductor resistance R_L , this parameter is strongly temperature-dependent. At room temperature (298 K), the copper coil typically exhibits higher resistance, which significantly decreases under cryogenic conditions (77 K) due to the reduction in copper resistivity. When superconducting inductors are employed, this resistance can be virtually eliminated. Consequently, temperature has a direct and substantial impact on the achievable voltage gain, as illustrated in Fig. 2, where larger R_L values correspond to room-temperature operation, and smaller values approximate cryogenic scenarios. This highlights the advantage of cryogenic operation in mitigating copper losses and enhancing converter performance.

Fig. 2 illustrates the theoretical static voltage gain for different values of inductor resistance R_L . As R_L increases, the voltage gain progressively decreases, with the most significant deviation occurring as the duty cycle d approaches unity. This behavior highlights the critical role of inductor

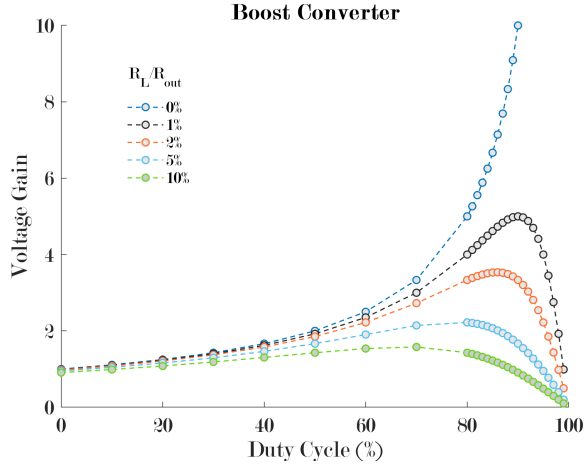


FIGURE 2. Theoretical voltage gain as a function of duty cycle, considering inductor copper losses modeled as a series resistance R_L .

copper losses in limiting the maximum attainable output voltage.

The model can be further improved by including losses in the diode D and semiconductor switch S_w . The gain equation of the boost DC–DC converter, considering these losses, is expressed as follows:

$$\frac{V_{out}}{V_{in}} = \left(\frac{1}{d'} \right) \left(1 - \frac{d' V_D}{V_{in}} \right) \left(\frac{1}{1 + \frac{R_L + dR_{SW} + d'R_D}{d'^2 R_{out}}} \right) \quad (9)$$

where:

- $d' = 1 - d$: Complement of the duty cycle;
- V_D : Voltage drop across the diode;
- R_L : Inductor resistance;
- R_{SW} : Switch resistance;
- R_D : Diode resistance;
- R_{out} : Equivalent load resistance.

When component losses are accounted for, the voltage conversion ratio is reduced, limiting the maximum achievable gain of the boost converter. These losses can be minimized through design and implementation techniques for power electronic converters in cryogenic environments. In such conditions, both magnetic components and semiconductors, when operating at cryogenic temperatures, exhibit reduced losses.

III. EXPERIMENTAL SETUP

This section presents the experimental procedures performed to validate the proposed high-gain cryogenic boost converter concept. Fig.3 presents the assembled boost converter test bench and the used equipments. The semiconductor devices employed are the Silicon Carbide (SiC) Power MOSFET C3M0045065K and the SiC Schottky Diode C6D20065A. The gate driver used is the CGD15SG00D2,

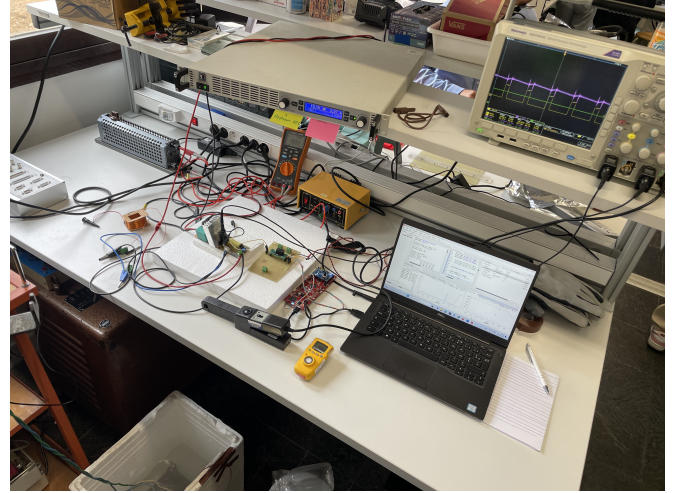


FIGURE 3. Experimental setup of the cryogenic boost converter.

an isolated single-channel driver designed for 3rd-generation SiC MOSFETs. The PWM driving signal is generated by the LAUNCHXL-F280049C microcontroller and transmitted to the gate driver. The measurements were acquired using a Tektronix MDO4034C scope and current probe A622. A 150 W prototype was developed to conduct a scaled-down analysis, aiming to assess the potential of using HTS inductors to enable higher power levels in boost converters.

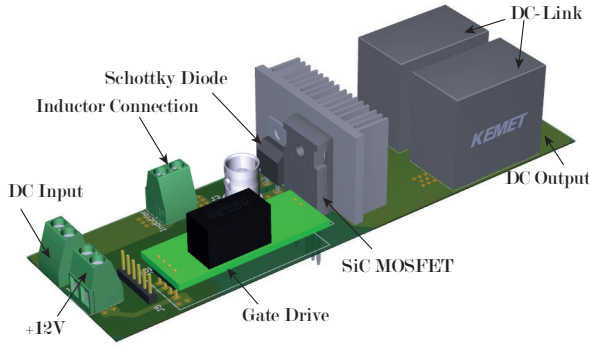
To minimize current ripple, the converter operates at a high switching frequency of 50 kHz. This allows the use of low-inductance coils (in the μH range), which reduces overall volume. Although current ripple at this frequency may lead to significant AC losses in the superconducting coil [34], this aspect will be investigated in future studies. Additionally, due to the high cost of superconducting tape, using a low inductance value enables a design with fewer turns, thereby reducing overall cost. The use of an air-core copper inductor also eliminates ferromagnetic losses, improving efficiency. For comparison purposes, the copper inductor was designed to achieve an inductance value approximately equal to that of the superconducting inductor.

To evaluate the boost converter, an open-loop configuration was implemented, and the output voltage behavior was observed while varying the duty cycle from 0% to 96%. Tests were conducted at room temperature (298 K = 25 °C) and in an open liquid nitrogen bath (77 K = -196 °C). For each temperature condition, two types of inductors were tested: a conventional copper air-core coil and an air-core inductor wound with 1G high-temperature superconducting tape (Sumitomo DI-BSCCO™ HT-CA tape). Additional experimental specifications are provided in Table 1. The developed boost converter prototype and the inductors used (HTS and copper) are shown in Figs.4 and 5, respectively.

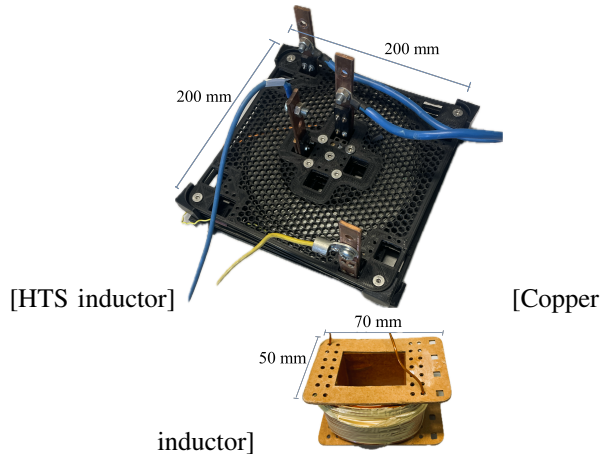
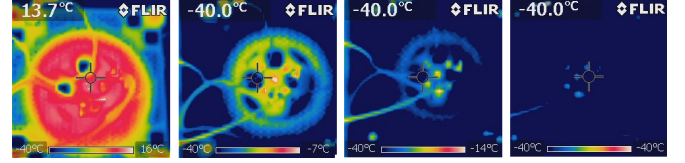
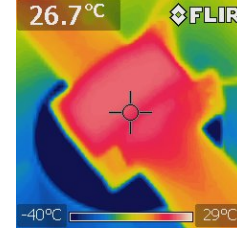
To ensure stable and repeatable cryogenic conditions during experimental evaluation, a controlled pre-cooling procedure was applied to the inductors to prevent damage caused by differential thermal contraction [36]. Initially,

TABLE 1. Experimental Component List and Parameters of the Boost Converter (Maximum Power: 150 W)

Parameters	Description	Value
V_{in}	Input Voltage	10 V
R_{out}	Resistive load	100 Ω
S_w	Silicon Carbide Power Mosfet	C3M0045065K
D	Silicon Carbide Schottky Diode	C6D20065A
G_D	Gate Driver	CGD15SG00D2
L_{HTS}	HTS coil	0.650 mH
L_{copper}	COPPER coil	0.675 mH , 0,497 Ω
C	Output capacitor	20 μ F
PWM generator	TI TMS320F280049C	100 MHz C28x
f_{sw}	Switching Frequency	50 kHz

**FIGURE 4. Developed boost converter board.**

the inductor was suspended a few centimeters above a polystyrene container filled with liquid nitrogen (LN_2) for approximately 10 minutes, allowing gradual thermal conditioning through cold vapor exposure. Subsequently, the inductor was lowered to near the LN_2 surface and held at that position for an additional 10 minutes. Finally, the inductor was fully immersed in the liquid nitrogen and maintained in that state for 10 more minutes to ensure uniform temperature distribution throughout the coil.

**FIGURE 5. Approximate dimensions of the tested inductors: HTS pancake inductor (a) [35] and copper air-core coil (b).****FIGURE 6. LN_2 pre-cooling of the HTS coil.****FIGURE 7. LN_2 Pre-Cooling of the copper coil.**

Figs. 6 and 7 show thermal camera images, capturing stages of the pre-cooling process for the HTS inductor and the copper coil, respectively. It is worth noting that the thermal camera cannot register temperatures below -40°C , which is the equipment's lower limit. However, once the components are fully immersed in liquid nitrogen, their equilibrium temperature reaches approximately 77 K.

IV. EXPERIMENTAL RESULTS

This section evaluates the performance of the boost converter operating with both the copper coil and the HTS superconducting coil, under room and cryogenic temperature conditions.

A. COPPER coil

Fig. 8 shows the measured voltage gain as a function of the duty cycle under five different test conditions, along with a simulated result for comparison. It is important to note that during the cryogenic tests, only the inductor was immersed in liquid nitrogen, while the PCB remained at room temperature. The purpose of testing under different load resistance values (R_{out}) is to demonstrate that the voltage gain depends not only on changes in the inductor resistance (R_L) but also on variations in the load, as shown in equation 8. The resulting curves are:

- 1) Experimental (room temperature) - T_0 condition;
- 2) Experimental (room temperature, post-stabilization) - T_1 condition;
- 3) Experimental (cryogenic, copper coil inside LN_2 bath, with varying load resistances) - $T_{cryo_{1,2,3}}$ condition;
- 4) Simulation (room temperature, with real parameters) - T_{SIM} condition;

The tests with the traditional copper inductor in a cryogenic environment showed promising results in terms of voltage gain, indicating that its performance closely approximates the ideal case. Therefore, cooling the inductor, even

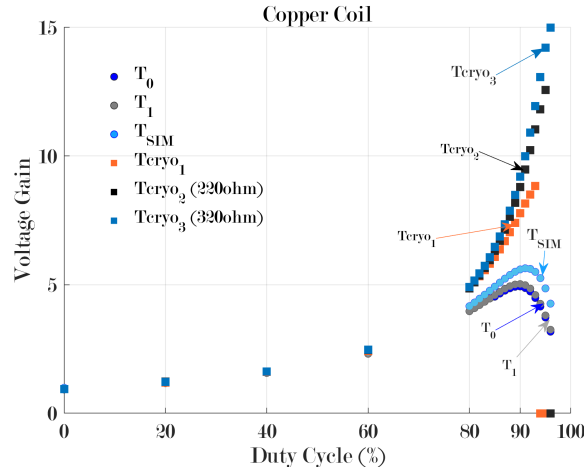


FIGURE 8. Results with copper coil. Measured and simulated voltage gain as a function of duty cycle at room and cryogenic temperatures under different conditions.

with copper wire, leads to a higher output voltage compared to the room temperature tests.

It is important to note that in these tests, the converter power was approximately 100 W. At higher power levels, with the same inductor design, the converter's gain is expected to decrease when using the air copper coil. In these cases, when the current is high, the use of the superconductor coil becomes more advantageous compared to the traditional copper coil.

B. HTS coil

Fig. 9 shows the measured voltage gain as a function of the duty cycle under four different conditions for the HTS coil. The simulation results are omitted, assuming that the superconducting inductor at room temperature exhibits an equivalent resistance to that of the copper inductor, resulting in similar behavior to Fig. 8. The following conditions were tested:

- 1) Experimental (room temperature) – T_0 condition;
- 2) Experimental (cryogenic, with only HTS coil inside LN_2 bath) – T_{cryo1} condition;
- 3) Experimental (cryogenic, with semiconductors and HTS coil inside LN_2 bath) – T_{cryo2} condition;
- 4) Experimental (cryogenic, with semiconductors, HTS coil, and SiC driver inside LN_2 bath) – T_{cryo3} condition.

As observed, the cryogenic boost converter demonstrates excellent voltage gain. As the series resistance of the inductor approaches zero, the gain increasingly aligns with the ideal case. Although testing HTS material at room temperature is uncommon, this was done to compare the effects of temperature on the series resistance of the superconducting inductor, since 1G HTS consists of BSCCO filaments embedded in a silver matrix. Moreover, no significant difference in gain improvement was observed between conditions T_1 and T_2 .

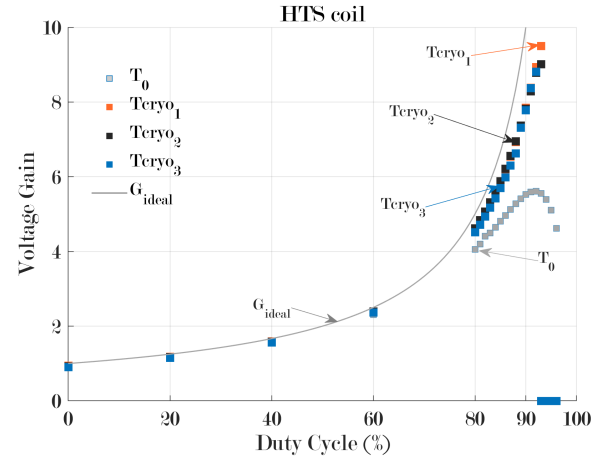


FIGURE 9. Results with HTS coil. Measured voltage gain as a function of the duty cycle at room and cryogenic temperatures under different conditions.

However, immersion of the semiconductors in liquid nitrogen may eliminate the need for a heatsink. Under condition T_3 , a slight reduction in gain is observed, which may constrain driver operation within an LN_2 environment.

Fig. 10 shows the typical steady-state boost converter experimental waveforms — output voltage, inductor current, and switch voltage — under T_1 conditions.

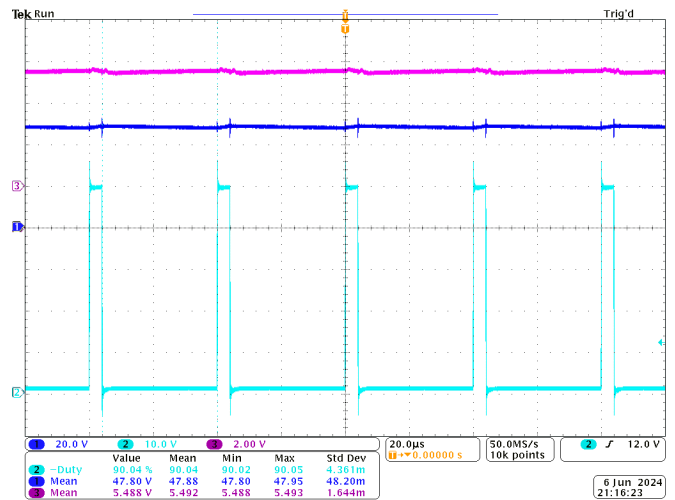


FIGURE 10. Output voltage, inductor current, and switch voltage for $d = 90\%$, $V_{in} = 10$ V, using HTS coil under T_1 condition.

Testing the converter in a cryogenic environment demonstrated promising results, aligning with expectations for high static gain converters. The reduced series resistance of the inductor significantly contributed to this improvement. Cooling the inductor and semiconductors yielded a higher output voltage gain compared to tests at room temperature.

While the use of high-temperature superconducting (HTS) inductors may appear excessive for general-purpose electronics, their application becomes relevant in niche scenarios that inherently demand cryogenic conditions and benefit

from minimized losses and compact magnetics. As discussed before, examples include aerospace systems, particle accelerators, quantum computing infrastructure, and superconducting energy storage devices. In such contexts, cryogenic infrastructure is already available, and HTS-based inductors can enable compact designs with extremely low conduction losses and enhanced efficiency. Although not intended for mass-market power supplies, the experimental results highlight the potential of HTS inductors as enabling components in high-performance cryogenic power converters.

V. CONCLUSION

This paper investigated the performance enhancement of a classical boost converter by replacing the conventional copper inductor operating at room temperature with a high-temperature superconducting (HTS) coil under cryogenic conditions.

Experimental results using the HTS coil confirmed the feasibility and effectiveness of the proposed approach. The measured waveforms were consistent with the expected behavior of a classical boost converter. As anticipated, the substantial reduction in series resistance provided by the HTS material led to a remarkable improvement in voltage gain, with the output voltage reaching nearly ten times the input voltage. This represents a significant enhancement compared to the conventional copper inductor, which achieved a maximum gain of approximately five times.

Additionally, the use of a copper inductor immersed in liquid nitrogen was evaluated as a cost-effective alternative. While this setup also showed improved voltage gain compared to operation at room temperature, its performance is limited under higher current conditions. In contrast, the HTS coil is expected to offer superior performance in high-power applications due to its enhanced conductivity and reduced losses under elevated current levels.

Future work related to operation in a cryogenic environment includes analysis of switching behavior for semiconductor characterization, implementation of closed-loop control for dynamic performance evaluation, investigation of steady-state behavior at different temperature levels in LN₂, and evaluation of efficiency curves along with a detailed study of losses.

Moreover, for the practical adoption of HTS and air-core inductors in cryogenic power electronics, future studies should perform a comprehensive trade-off analysis considering electrical performance alongside size, cost, cooling infrastructure requirements, and overall system complexity. Such an evaluation would provide a clearer understanding of the applicability and challenges of these technologies in various real-world scenarios.

AUTHOR'S CONTRIBUTIONS

S.A.MUSSA: Conceptualization, Data Curation, Formal Analysis, Investigation, Methodology, Project Administration, Resources, Software, Supervision, Validation, Visu-

alization, Writing – Original Draft, Writing – Review & Editing. **H.M.O.FILHO:** Data Curation, Formal Analysis, Investigation, Methodology, Validation, Writing – Original Draft, Writing – Review & Editing. **G.A.L.HENN:** Data Curation, Formal Analysis, Investigation, Methodology, Visualization, Writing – Original Draft, Writing – Review & Editing. **D.M.SOTORIVA:** Data Curation, Software, Visualization. **L.FERREIRA:** Data Curation, Investigation, Validation, Visualization. **L.QUEVAL:** Conceptualization, Data Curation, Formal Analysis, Funding Acquisition, Investigation, Methodology, Project Administration, Resources, Supervision, Validation, Visualization, Writing – Original Draft, Writing – Review & Editing.

PLAGIARISM POLICY

This article was submitted to the similarity system provided by Crossref and powered by iThenticate – Similarity Check.

DATA AVAILABILITY

The data used in this research is available in the body of the document.

REFERENCES

- [1] A. Karbowniczak, H. Latala, K. Necka, S. Kurpaska, L. Ksiazek, “Modelling of Energy Storage System from Photoelectric Conversion in a Phase Change Battery”, *Energies*, vol. 15, no. 3, 2022, doi:10.3390/en15031132, URL: <https://www.mdpi.com/1996-1073/15/3/1132>.
- [2] A. Russo, A. Cavallo, “Stability and Control for Buck–Boost Converter for Aeronautic Power Management”, *Energies*, vol. 16, no. 2, 2023, doi:10.3390/en16020988, URL: <https://www.mdpi.com/1996-1073/16/2/988>.
- [3] H. Li, Y. Gu, X. Zhang, Z. Liu, L. Zhang, Y. Zeng, “A Fault-Tolerant Strategy for Three-Level Flying-Capacitor DC/DC Converter in Spacecraft Power System”, *Energies*, vol. 16, no. 1, 2023, doi:10.3390/en16010556, URL: <https://www.mdpi.com/1996-1073/16/1/556>.
- [4] J. Zhang, S. Yang, F. C. Lee, Q. Li, “High Efficiency DC–DC Converter Design for Data Centers With 48 V Power Distribution”, *IEEE Transactions on Power Electronics*, vol. 32, no. 6, pp. 4726–4739, 2017, doi:10.1109/TPEL.2016.2599218.
- [5] V. J. Samuel, G. Keerthi, P. Mahalingam, “Coupled inductor-based DC–DC converter with high voltage conversion ratio and smooth input current”, *IET Power Electronics*, vol. 13, pp. 733–743, 2020, doi:10.1049/iet-pel.2019.0933.
- [6] A. Farakhori, M. Abapour, M. Sabahi, “A Study on the Derivation of the Continuous Input Current High Voltage Gain DC/DC Converters”, *IET Power Electronics*, vol. 11, 03 2018, doi:10.1049/iet-pel.2017.0687.
- [7] F. Sedaghati, S. Pourjafar, “Analysis and implementation of a boost DC–DC converter with high voltage gain and continuous input current”, *IET Power Electronics*, vol. 13, pp. 798–807, 2020, doi:10.1049/iet-pel.2019.0973.
- [8] G. A. L. Henn, R. N. A. L. Silva, P. P. Praça, L. H. S. C. Barreto, D. S. Oliveira, “Interleaved-Boost Converter With High Voltage Gain”, *IEEE Transactions on Power Electronics*, vol. 25, no. 11, pp. 2753–2761, 2010, doi:10.1109/TPEL.2010.2049379.
- [9] R. Middlebrook, “Transformerless DC-to-DC converters with large conversion ratios”, *IEEE Transactions on Power Electronics*, vol. 3, no. 4, pp. 484–488, 1988, doi:10.1109/63.17970.
- [10] B. Zhao, Q. Song, W. Liu, Y. Sun, “Overview of Dual-Active-Bridge Isolated Bidirectional DC–DC Converter for High-Frequency-Link Power-Conversion System”, *IEEE Transactions on Power Electronics*, vol. 29, no. 8, pp. 4091–4106, 2014, doi:10.1109/TPEL.2013.2289913.
- [11] B. Andres, L. Romitti, A. M. S. S. Andrade, L. Roggia, L. Schuch, “A High Step-Up Isolated DC-DC Converter Based on Cascaded Greinacher Voltage Multiplier”, *Revista*

- Eletrônica de Potência*, vol. 28, no. 1, pp. 52–62, February 2023, doi:10.18618/REP.2023.1.0038, URL: <https://journal.sobraep.org.br/index.php/rep/article/view/913>.
- [12] G. E. R. da Silva, C. M. de O. Stein, J. P. da Costa, E. G. Carati, R. Cardoso, G. W. Denardin, J. B. B. Quispe, “An Isolated Active-Clamped Circuit Current-Fed Half-Bridge Converter”, *Eletrônica de Potência*, vol. 30, p. e202522, February 2025, doi:10.18618/REP.e202522, URL: <https://journal.sobraep.org.br/index.php/rep/article/view/1008>.
 - [13] F. L. de Sá, D. Ruiz-Caballero, S. A. Mussa, “A new DC-DC double Boost Quadratic converter”, in *2013 15th European Conference on Power Electronics and Applications (EPE)*, pp. 1–10, 2013, doi:10.1109/EPE.2013.6634441.
 - [14] F. L. de Sá, C. D. Agnol, D. A. Ruiz-Caballero, S. A. Mussa, “Análise Estática e Dinâmica do Conversor CC-CC Duplo-Buck Quadrático”, *Eletrônica de Potência*, vol. 26, pp. 53–63, 3 2021, doi:10.18618/rep.2021.1.0056.
 - [15] F. Lima de Sa, C. Dal Agnol, W. Raphael, D. R. Caballero, S. A. Mussa, “A New DC-DC Double Zeta Quadratic Converter”, in *2020 IEEE International Conference on Industrial Technology (ICIT)*, pp. 426–431, 2020, doi:10.1109/ICIT45562.2020.9067314.
 - [16] F. L. de Sá, D. Ruiz-Caballero, C. Dal’Agnol, W. R. da Silva, S. A. Mussa, “High Static Gain DC-DC Double Boost Quadratic Converter”, *Energies*, vol. 16, no. 17, p. 6362, Sep. 2023, doi:10.3390/en16176362, URL: <https://doi.org/10.3390/en16176362>.
 - [17] W. R. da Silva, F. L. de Sá, C. Dal Agnol, S. A. Mussa, “High-gain Differential Quadratic Boost DC-DC Converter”, in *2023 IEEE 8th Southern Power Electronics Conference and 17th Brazilian Power Electronics Conference (SPEC/COBEP)*, pp. 1–8, 2023, doi:10.1109/SPEC56436.2023.10407860.
 - [18] C. Dal Agnol, F. L. de Sa, W. R. da Silva, S. A. Mussa, “High Static Gain Boost-Ćuk DC-DC Converter”, in *2023 IEEE 8th Southern Power Electronics Conference and 17th Brazilian Power Electronics Conference (SPEC/COBEP)*, pp. 1–8, 2023, doi:10.1109/SPEC56436.2023.10408370.
 - [19] W. R. da Silva, F. L. de Sá, C. Dal Agnol, S. A. Mussa, “High-gain Differential Quadratic Boost DC-DC Converter”, in *2023 IEEE 8th Southern Power Electronics Conference and 17th Brazilian Power Electronics Conference (SPEC/COBEP)*, pp. 1–8, 2023, doi:10.1109/SPEC56436.2023.10407860.
 - [20] M. Forouzesh, Y. P. Siwakoti, S. A. Gorji, F. Blaabjerg, B. Lehman, “Step-Up DC-DC Converters: A Comprehensive Review of Voltage-Boosting Techniques, Topologies, and Applications”, *IEEE Transactions on Power Electronics*, vol. 32, no. 12, pp. 9143–9178, 2017, doi:10.1109/TPEL.2017.2652318.
 - [21] Y. Pontes, C. E. de Alencar e Silva, E. M. S. Junior, “High-Voltage Gain DC-DC Converter For Photovoltaic Applications In DC Nanogrids”, *Eletrônica de Potência*, vol. 25, no. 4, pp. 473–480, December 2020, doi:10.18618/REP.2020.4.0021, URL: <https://journal.sobraep.org.br/index.php/rep/article/view/305>.
 - [22] J. C. Dias, T. B. Lazzarin, “Boost DC-DC Converter with Switched-Capacitor and Four-State Switching Cell”, *Eletrônica de Potência*, vol. 27, no. 3, pp. 267–278, January 2024, doi:10.18618/REP.2022.3.0023, URL: <https://journal.sobraep.org.br/index.php/rep/article/view/135>.
 - [23] Y. Lee, J. Park, G. Cho, H. Kim, “Design of a Cryogenic Power Converter for Space Applications”, *IEEE Transactions on Aerospace and Electronic Systems*, vol. 54, no. 2, pp. 644–653, 2018, doi:10.1109/TAES.2017.2775238.
 - [24] T. Kawahara, H. Takahashi, K. Hamada, “Development of a Cryogenic Power Supply for the Superconducting Magnet System of a Fusion Device”, *IEEE Transactions on Applied Superconductivity*, vol. 20, no. 3, pp. 540–543, 2010, doi:10.1109/TASC.2009.2038582.
 - [25] A. O. Orlov, S. V. Rylov, V. K. Kornev, “Cryogenic Electronics: From Quantum Computing to High-Speed Digital and Mixed-Signal Applications”, *IEEE Transactions on Applied Superconductivity*, vol. 29, no. 5, pp. 1–6, 2019, doi:10.1109/TASC.2019.2901522.
 - [26] C. Wang, Z. Xu, J. Liu, Y. Zhang, “Development of a 10 kJ HTS SMES System With Full Power Converter”, *IEEE Transactions on Applied Superconductivity*, vol. 23, no. 3, p. 5700204, 2013, doi:10.1109/TASC.2012.2237410.
 - [27] S. A. Sattar, A. B. Lostetter, P. L. Palmer, S.-H. Ryu, B. J. Baliga, “SiC Power Devices at Cryogenic Temperatures”, *IEEE Transactions on Industry Applications*, vol. 40, no. 6, pp. 1594–1602, 2004, doi:10.1109/TIA.2004.836218.
 - [28] M. W. El-Kharashi, M. M. A. Salama, M. El-Chamie, “Cryogenic Power Electronics: A Review”, *IEEE Transactions on Applied Superconductivity*, vol. 26, no. 7, pp. 1–5, 2016, doi:10.1109/TASC.2016.2586039.
 - [29] M. Arfaoui, Y. Wang, E. F. Fuchs, “A Survey of Power Semiconductor Devices at Cryogenic Temperatures”, *IEEE Transactions on Industrial Electronics*, vol. 67, no. 9, pp. 7453–7462, 2020, doi:10.1109/TIE.2019.2931221.
 - [30] C. Sankaran, “Air-Core Inductors in High-Frequency Applications: Advantages and Limitations”, *IEEE Trans Magnetics*, vol. 39, no. 4, pp. 2020–2025, 2003, doi:10.1109/TMAG.2003.814072.
 - [31] C. A. Luongo, et al., “Superconducting devices for power systems: the state of the art and perspectives”, *IEEE Trans Appl Supercond*, vol. 11, no. 1, pp. 1450–1458, 2001, doi:10.1109/77.919422.
 - [32] A. Rajendra, V. Selvamani, R. E. Koritala, “Design Considerations for HTS-based Inductors in Power Electronic Converters”, *IEEE Trans Appl Supercond*, vol. 30, no. 4, pp. 1–6, 2020, doi:10.1109/TASC.2020.2967496.
 - [33] R. Erickson, D. Maksimovic, *Fundamentals of Power Electronics*, Online access with purchase: Springer, Springer US, 2001, URL: https://books.google.com.br/books?id=S91G_Nz_KjEC.
 - [34] H. Liu, G. Song, W. Feng, M. Qiu, J. Zhu, S. Rao, “Experimental and Simulation Research of AC Ripple Losses in a High Temperature Superconductor Tape”, *Advances in Condensed Matter Physics*, vol. 2018, p. 1904817, 2018, doi:10.1155/2018/1904817.
 - [35] R. Coelho-Medeiros, L. Queval, J. Dai, J.-C. Vannier, P. Egrot, “Integration of HTS Coils in a Lab-Scale Modular Multilevel Converter”, *IEEE Transactions on Applied Superconductivity*, vol. 32, no. 4, pp. 1–4, 2022, doi:10.1109/TASC.2022.3168255.
 - [36] H.-M. Chang, Y. S. Choi, S. W. V. Sciver, T. L. Baldwin, “Cryogenic Cooling Temperature of HTS Transformers for Compactness and Efficiency”, *IEEE Transactions on Applied Superconductivity*, vol. 13, no. 2, pp. 2298–2301, June 2003, doi:10.1109/TASC.2003.812748.

BIOGRAPHIES

Samir Ahmad Mussa received the degree of Electrical Engineer from the Federal University of Santa Maria in 1988, he received the Master’s and Doctor’s degrees from the Federal University of Santa Catarina in 1994 and 2003 respectively. He currently holds the position of Full Professor in the Department of Electrical and Electronic Engineering (EEL) at the Federal University of Santa Catarina (UFSC) and researcher at the Institute of Power Electronics (INEP). His research interests include PFC rectifiers, digital signal processing and control applied in power electronics, DSP-based systems, FPGA and microprocessors, cryogenic power electronics and superconductor applications. Dr. Mussa is a member of the Brazilian Society of Power Electronics (SOBRAEP) and the IEEE.

Herminio Miguel de Oliveira Filho was born in Taguatinga, Distrito Federal, Brazil, in 1983. He received B.Sc., M.Sc. and D.Sc. degrees in electrical engineering from the Federal University of Ceara; (UFC), Fortaleza, Brazil, in 2007, 2010 and 2015, respectively. Currently, he is a professor and a researcher in the Electrical Energy Processing and Planning Group (GProPEE) in the University for the International Integration of the Afro-Brazilian Lusophony (UNILAB), Redenção, Brazil, and also a researcher in the Power Processing and Control Group (GPEC) in the UFC. His interest areas include control applications in power electronics, bidirectional dc-dc converters, energy storage systems and renewable energy applications. Prof. Oliveira Filho is a Member of the Brazilian Power Electronics Society (SOBRAEP) and IEEE Power Electronics Society (PELS).

Gustavo Alves de Lima Henn was born in Fortaleza-CE, Brazil, in 1983. He received the BSc, MSc, and PhD degrees in electrical engineering from Federal University of Ceará, Brazil, in 2006, 2008, and 2012 respectively. In 2022 completed the Postdoctoral fellowship in the University Paris-

Saclay, France. He is currently researcher in the Group of Electrical Energy Processing, and associated professor at the University of International Integration of Afro-Brazilian Lusophony, Redenção/CE, Brazil. His interest fields include static power converters, renewable energy applications, multilevel converters, and power electronics cryogenic applications.

Douglas Mendes Sotoriva was born in Vacaria, Rio Grande do Sul, Brazil, in 1997. He received his Bachelor's degree in Electrical Engineering from Centro Universitário Facvest (Unifacvest) in 2020 and is currently pursuing a Master's degree in Power Electronics at the Federal University of Santa Catarina (UFSC). His research interests include power electronics, AC–DC converters and wide bandgap semiconductors (SiC and GaN).

Lauro Ferreira was born in Resende, RJ, Brazil, in 1994. He received his B.Sc. degree in Electrical Engineering from the Federal University of Rio

de Janeiro, Brazil, in 2019, and his M.Sc. degree in Intelligent Electric Vehicles from the University of Lille, France, in 2021. He is currently pursuing a Ph.D. in Electrical Engineering within the GeePs (Group of Electrical Engineering of Paris) at CentraleSupélec, Université Paris-Saclay, France. His research interests include power systems, power electronics, superconducting applications, and electric mobility.

Loïc Queval received the Ph.D. degree in science from the University of Tokyo, Tokyo, Japan, in 2013. He is currently Full Professor in the GeePs Laboratory, CNRS, CentraleSupélec, Univ. Paris-Saclay, Sorbonne University, Gif sur Yvette, France. His main research interests include energy systems, electrical machines and applied superconductivity.